e-Polymers **2006**, no. 014

http://www.e-polymers.org
ISSN 1618-7229

Effect of organoclay impurities on mechanical properties of EVA-layered silicate nanocomposites

Bellucci F.[1], Camino G.[1], Frache A.[1], Ristori V.[1], Sorrentino L.[2], Iannace S.[2], Bian X.[3], Guardasole M.[3], Vaccaro S.[3,4]*

[1*] Centro di Cultura per l'Ingegneria delle Materie Plastiche, Politecnico di Torino sede di Alessandria, INSTM Unit Research, V. Teresa Michel 5 15100 Alessandria. e-mail:alberto.frache@polial.polito.it
[2] Institute for Composite and Biomedical Materials (IMCB-CNR), Piazzale E. Fermi 1 - 80055 Portici (NA), Italy
[3] Elcon Megarad Srl, via Arrigo Cavaglieri 26, 00173 Roma
[4] ENEA —CR Casaccia, Via Anguillarese 301 - 00060 S. Maria di Galeria (Roma)

(Received: 3 November, 2005; Published: 10 May, 2006)

Abstract: The purification process of commercial organoclays and the beneficial effect of the impurities removal on the mechanical properties of the EVA exfoliated and intercalated nanocomposites are described in this paper. Mechanical properties such as Young modulus are improved, without any change in morphology in the exfoliated nanocomposites and an improvement of intercalation degree in the intercalated nanocomposite as demonstrated by rheological test is observed.
Keywords: nanocomposites, washing process, thermal analysis, rheological test.

Introduction

Polymeric nanocomposites represent a fundamental step in the polymeric materials development [1]. Owing to the nanoscopic interaction between the polymer matrix and the filler, polymer nanocomposites could be considered organic/inorganic hybrids, showing a general substantial improvement in properties, such as mechanical and barrier properties, flame retardancy, etc. with low loading (<5%) of inorganic filler [2-4].

A typical example of this class of materials is that of polymer layered silicate nanocomposites (PLSN). The crystal structure of layered silicates, such as clays that are widely used to prepare PLSN, consists of two-dimensional layers (thickness ~ 0,96 nm) formed by fusing two silica tetrahedral sheets with an edge-shared octahedral sheet of either alumina or magnesia. Stacking of these layers leads to van der Waals' galleries. These galleries are occupied by cations, typically Na^+ and Ca^{2+}, which balance the charge deficiency generated by isomorphous substitution within the layers (e.g. tetrahedral Si^{4+} by Al^{3+} or octahedral Al^{3+} by Mg^{2+})[5-6].

A prerequisite for optimal PLSN composite properties is a good dispersion (deagglomeration and exfoliation) and spatial distribution of the filler layers in the matrix, which require optimal wetting of the filler galleries surface. Thus, the interface between the clay mineral and the polymer matrix is of crucial importance for morphology of the composites. Clay minerals have high-energy hydrophilic surfaces, which are incompatible with the low-energy hydrophobic polymer surface. For this

reason and to increase the interlamellar gap size, the clay minerals are treated with organic molecules [7].
The surface modification of the commercial clays with organic molecules is typically achieved via ion exchange reaction of the naturally occurring alkali metal cations residing between the aluminosilicate layers using alkylammoniun halides (generally chlorides or bromides). Products of this exchange reaction are: the organically modified clay (organoclay), the unreacted alkylammonium and sodium halides that are washed out at the end of the ion-exchange process. Commercial clays contain residual impurities of alkylammonium and sodium halides which may badly affect the final properties of nanocomposites [8-10].

In this paper we describe a washing process of two commercial organoclays and the beneficial effect of purification on the mechanical properties in the nanocomposites obtained with the purified organoclays.

Experimental Section

Materials

The ethylene vinyl acetate copolymer used is a copolymer that contains 19 wt% of vinyl acetate, (Escorene Ultra FL00119, Exxon Mobil Chemical. Melting point 84°C ,density 0.942 g/cm^3) The commercial organoclays used are Somasif MEE, a synthetic fluorohectorite exchanged with $[CH_3]$ [HT] $[CH_2O]_xH$ $[CH_2O]_yH$ N^+ (where x + y = 2), a methyl hydrogenated tallow, dihydroxyalkyl ammonium ion, produced by UNICOOP Japan, and Nanofil 15 a natural montmorillonite exchanged with $[CH_3]_2$ $[HT]_2$ N^+, a di-methyl di-hydrogenated tallow ammonium ion, produced by Süd Chemie.

Washing process of commercial clays

In a 1l round bottom flask equipped with a mechanical stirrer (70 rpm) 40g of clay were wetted with 100cc of EtOH and added with 900cc of deionized water (<10µS). The suspension was stirred for two hours, 60°C. The suspension was filtered on a Buchner, washed on the filter with 3l of hot deionized water. After this treatment, residual chlorides or bromides were revealed by suspending 1g of washed clay into 10cc of deionized water, stirring at 60°C for 30min, filtering and treating the filtrate with 1cc of 0.1M $AgNO_3$. The procedure was generally successful; however, if halides were still present, the entire washing process is repeated until halides are no more evident with $AgNO_3$ test. As soon as the halides are removed the filtrated clay is pressed on the Buchner in order to eliminate the most of water contained in the wet clay, and then it is dried in a vacuum oven at 80°C for 12h. When the drying process is ended the clay is pulverized using sequentially a grinder and a mortar.

Compounding and preparation of EVA nanocomposites

EVA nanocomposites were prepared with original and purified organoclays using an internal mixer, Brabender W50E.EVA and 5wt% of clay were melt blended at 125°C-130°C, rotor speed 60 rpm, residence time 3 min.

Characterization

Thermogravimetry (TG) was performed on a TA instrument Q500 thermobalance with a heating ramp of 10°C/min from 50°C to 800°C both in nitrogen and air (60cm^3/min). The analysis was performed in triplicate for each sample.

Morphology of organoclays and EVA nanocomposites, was characterized by ARL X'TRA 48 X Ray diffractometer.
The rheological measurements were performed in an oscillatory shear mode using a 25mm parallel plate geometry under nitrogen flow, by using a Rheometric Scientific ARES rotational rheometer.

Samples were tested at 210°C by using a dynamic frequency sweep test, with frequency ranging from 0.01 to 15 Hz and strain fixed to 1%, in order to assure to stay in the linear viscoelastic range (determined by a time sweep test at 210°C).
The thermal degradation effects during the experimental time are found to be negligible.

Mechanical testing was performed using an Instron Dynamometer model 4202. Specimens, 1 mm thick, were prepared and tested according to ASTM D1708 standard.

Results and discussion

Thermal behaviour of purified clay

Thermal decomposition of the organic modifier in the organoclay Nanofil 15 occurs in two main steps between 200°C and 500°C, as shown in Figure 1 A (solid line). The first step, that is in correspondence of the shoulder at 248°C (±5°C) (Figure 1 A DTG solid line), is due to the decomposition of the unconfined fraction of alkyl ammonium, that consists of alkyl ammonium halide surfactant which has not undergone the ion exchange reaction and is present in the organoclay in one or more of the following position: either complexed outside the interlamellar galleries or within void spaces between primary particles or inside the interlayers but in a peripheral position[9]. The main products released during this first degradation process are long olefin chains and amines that suggest that Hoffman elimination reaction takes place [9]. Inside the interlayer spaces, instead, the initial decomposition products diffusion to the gas phase is made difficult by the barrier effect of the clay layers, thus these products are trapped and, at higher temperatures, they undergo further reactions producing small molecular weight species which are released in the second step of degradation between 300°C and 500°C with a maximum rate of weight loss at 314°C (±5°C) [9-10].

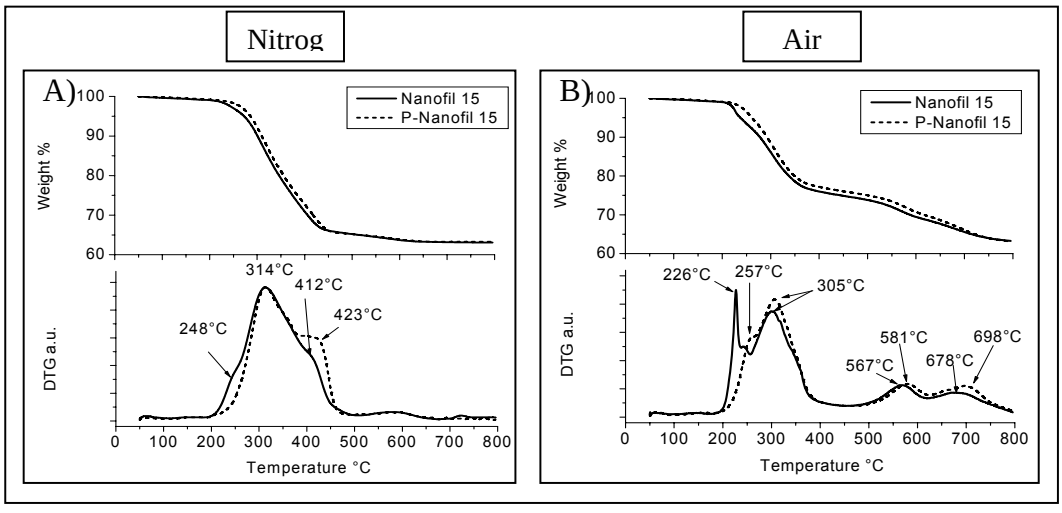

Fig. 1. TGA and DTG in inert (A) and oxidative (B) atmosphere of Nanofil 15 (——) and P-Nanofil 15 (- - - -).

During the degradation carried out in air the unconfined alkylammonium ions are exposed to the action of the air that increase the rate of their degradation (T max. 226°C (±5°C), Figure 1 B, solid line, DTG max ca. 0.2 %weight loss/°C) as compared to nitrogen (Figure 1, shoulder at 248°C (±5°C), DTG max 0.07 %weight loss/°C) with a difference of about 20°C in temperature of maximum weight loss. Whereas, the intercalated fraction of alkylammonium ion is partially sheltered from the action of oxygen by the barrier action of the clay layers and decomposes to volatiles with maximum rate at 302°C that is only 11°C below the temperature of maximum weight loss rate in nitrogen. Partial charring of the alkylammonium ion is induced in air by the contact with the clay as shown by the larger residue in figure 2 at the end of the main volatilisation process in air (70% at 400°C) as compared to nitrogen (63% at 480°C). A two step char oxidation process takes place in air between 500-800°C which leads to a final inorganic residue that is the same as in nitrogen: 63%. Delayed thermal oxidation and charring of organic polymers nanocomposites on heating in air has been previously reported and a mechanism based on oxidative dehydrogenation of organic structures, catalysed by the clay was proposed [11-13].

In the thermogravimetric curves of purified Nanofil 15 (P-Nanofil 15) in nitrogen and air (Figure 1 A and B respectively) the weight loss due to the unconfined species has disappeared showing that the washing procedure besides sodium halide has also removed the excess of organic modifier. Since the total weight loss of original and purified organoclay is the same, it appears that during the washing procedure, the adsorbed organic modifier is intercalated within the clay galleries. Indeed, an increase of the shoulder appears in the high temperature range of the derivative thermogravimetric curve (423°C ±5°C) in nitrogen of the P-Nanofil 15 which should be due to a rearrangement of the intercalated material with further ion exchange and/or improvement of intercalation of the organic moieties within the barrier forming clay layers. This is in agreement with the shift towards higher temperatures of the weight loss process of the purified organoclay in air (Figure 1, e.g. peak at 226°C to shoulder at 257°C, peak at 302°C to 305°C) because of a more effective oxygen shielding action of the clay layers barrier. A similar thermal behaviour both in nitrogen and air was found for commercial and purified Somasif MEE (P-Somasif MEE).

Morphology of EVA nanocomposites

The XRD profiles of the original organoclays and of EVA nanocomposites are shown in Figures 2-3. In the case of Somasif MEE, which contains a polar organomodifier that is well compatible with the polymer chains, melt blending leads to an exfoliated nanocomposite with both the original and purified organoclay: in fact the absence of peaks in the XRD spectrum (Figure 2) in the 2θ range from 1° to 15° suggests that the clay loses its ordered structure. Whereas Nanofil 15 gives ordered intercalated nanocomposites by melt blending with EVA, because of its low polarity [14], with some differences in the XRD pattern depending on whether the original or purified organoclay is used (Figure 3). In the case of the original Nanofil 15, an increase of the interlayer distance from 3,1nm (2θ = 2,9°) to 4,1nm (2 θ = 2,2°)(001 first order diffraction) and second order peak at 2 θ = 4,4° can be observed. Instead, in the nanocomposite with P-Nanofil 15, the first order diffraction peak is at 2 θ =2,4°, which means an interlayer distance of 3,6nm. However, operating in the same experimental conditions, the signal of the first peak of purified clay-nanocomposite (4500 cps) is lower respect to the original clay nanocomposite (9000 Cps). This

could suggest that an amount of organoclay shows a quite low increment of the interlayer distance (from 3,1° to 3,6°) while same amount of the clay can have a higher level of intercalation, moving the first order diffraction peak to smaller angles not detectable by the instrument. The hypothesis of a better dispersion is supported by rheological data as discussed hereafter.

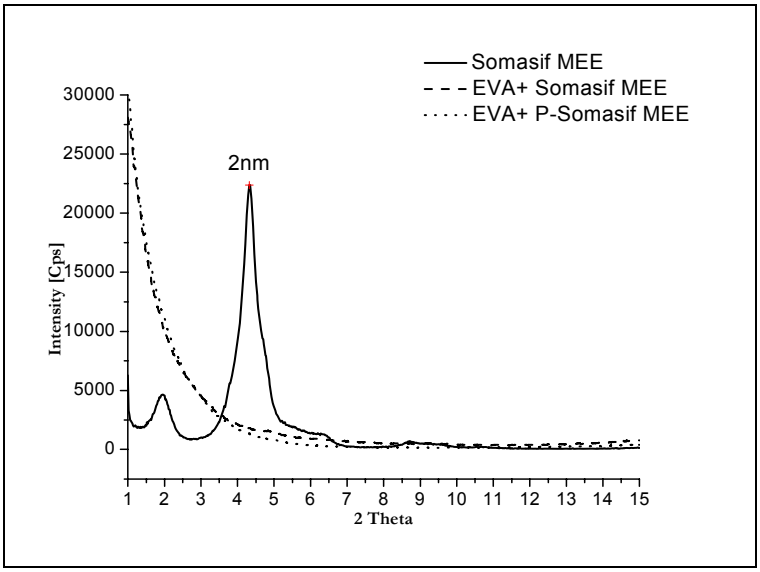

Fig. 2. Comparison between XRD patterns of Somasif MEE (——) and nanocomposites of EVA with 5 wt% of Somasif MEE (- - - - -) and P-Somasif MEE (·····).

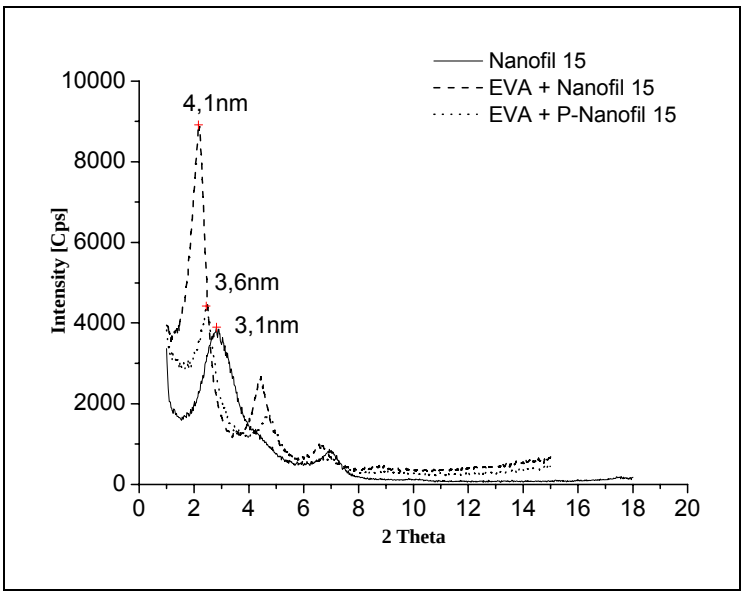

Fig. 3. Comparison between XRD patterns of Nanofil 15 (——)and nanocomposites of EVA with 5 wt% of Nanofil 15 (- - - - -) and P-Nanofil 15 (·····).

Rheology

The effect of the nanoparticles purification process on the degree of intercalation and/or exfoliation in the nanocomposites can be more conveniently shown by using rheological tests. The use of melt rheology to characterize polymer-clay nano composites has been widely used and different models have been utilized to quantify the degree of exfoliation/intercalation on the clay in the polymeric matrix [15-26]. Intercalation and/or exfoliation process both induce the appearance of shear-thinning effects, more apparent as the dispersion of the nanoparticles is more effective in the polymer matrix, and viscosity curves is more shifted towards higher values, at low shear rates. In several cases, the presence of clay leads to Bingham type materials, characterized by the presence of a yield stress. This means that flow cannot occur below a stress threshold. The yield stress model is based on the assumption that the unlimited increase of the viscosity when the shear rate goes to zero is caused by the presence of a network structure in the melt that leads to a yield stress. This can be caused by the dispersed particles, which can touch or connect to each other to form a continuous structure. The formation of a network does not require a physical connection between the particles, but it is sufficient that the particles feel each other's presence and are able to transfer stresses. Due to their large aspect ratio, the space the exfoliated silicate layers need to rotate freely in the melt is much larger than the volume they occupy. Therefore, the percolation threshold of exfoliated layered silicates is very low [27-28].

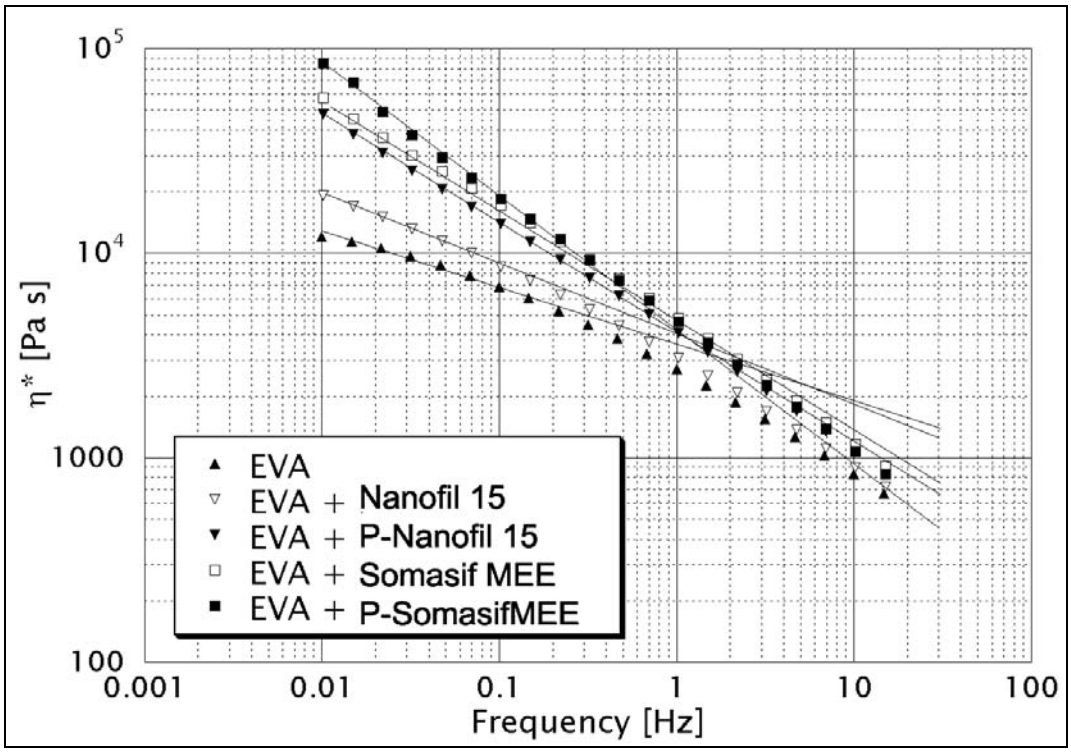

Fig. 4. Comparison between η* vs frequency behaviours of pure EVA ( ) and of the nanocomposites with Nanofil 15 ( ), P-Nanofil ( ), Somasif MEE ( ) and P-Somasif MEE ( ).

Tab. 1. Power law parameters, obtained by rheological curves of nanocomposites (R is the regression confidence).

Composition	*A*	*n*	R
EVA	4483	-0.218	0.9912
EVA + Nanofil 15	4159	-0.335	0.9994
EVA + P-Nanofil15	3809	-0.552	0.9997
EVA + Somasif MEE	4720	-0.543	0.9986
EVA + P-Somasif MEE	3554	-0.695	0.9981

According to Wagener and Reisinger [15], a useful method to quantitatively compare the degree of intercalation/exfoliation of nanocomposites is to use the power law equation and evaluate the slope of the regression line for the lower shear rates data in the plot of complex viscosity vs frequency.

In figure 4 is shown the effect of nanoparticles purification on the complex viscosity of all nanocomposite samples. Both for purified-N15 and purified MEE nanoparticles, the curves are shifted to higher values. The purification effect on rheology is very clear at very low shear rates, where the purified clay nanocomposites exhibit higher complex viscosity compared to that of non purified clay nanocomposites. As can be seen in figure 4, the low frequency data have been analyzed by using the power law regression model:

$$\eta^* = A\omega^n \tag{1}$$

with η^* as apparent complex viscosity, A as a sample specific pre exponential factor (theoretically corresponding to a viscosity value near that measured at ω=1 Hz), ω as the oscillation frequency of the rheometer equivalent to shear rate, n as the shear thinning exponent [15].

Tab. 2. Rheological parameters obtained with yield stress model.

Composition	η_0 [Pa s]	τ_0 [Pa]
EVA	12.5 10^3	---
EVA + Nanofil 15	16.4 10^3	50.0
EVA + P-Nanofil 15	24.8 10^3	275.5
EVA + Somasif MEE	24.6 10^3	360.1
EVA + P-Somasif MEE	135.0 10^3	412.8

In order to find n values, the regression equation Eq. 1 has been applied to low shear rates data in a log(η)-log(ω) plot and the regression lines are represented in Figure 4. As summerized in Table 1, n values are decreasing, due to the fact that the rheological curve slope at low frequency is higher for materials with a higher degree of intercalation/exfoliation. This analysis demonstrates the improving effect on the intercalation/exfoliation process of the nanoparticles purification process. This effect is more evident for the intercalated nanocomposite, in fact in this case, the improvement of EVA - P-Nanofil 15 nanocomposite n value is about 65% with

respect to the EVA – Nanofil 15 nanocomposite one. These data confirm the behaviour based on the XRD analysis.

The following yield stress model was also used to quantify the degree of exfoliation/intercalation of the nanocomposites:

$$\eta^* = \frac{\eta_o^*}{\left[1+\lambda\omega\right]^m} + \frac{\tau_o}{\omega} \qquad (2)$$

and the results, in terms of η_0 and τ_0 are reported in Table 2. The great variations of τ_0 for the different nanocomposites suggest that this model is more suitable than the power law model (Eq. 1) to quantify the degree of exfoliation/intercalation of clay. It is interesting to notice that the presence of a yield stress was observed only for nanocomposites and not for the pure EVA. Moreover, the zero shear viscosity η_0 was not affected as much as the yield stress τ_0 by the presence of nanoclay, except for the nanocomposite containing P-Somasif MEE 5%, showing also the highest yield stress. The τ_0 data suggest that purification of clay lead to nanocomposites with a higher network structure.

Mechanical properties of EVA nanocomposites

The results of mechanical tests are reported in Table 3. The Young modulus of the nanocomposites prepared with commercial organoclays was substantially improved relative to the neat EVA, whereas both elongation and stress at break were always lower. The Young modulus of the nanocomposites based on the Somasif MEE were higher than those based on Nanofil 15 and this can be attributed to the better dispersion of organoclay platelets of Somasif MEE in the polymeric matrix. Similar behavior has been reported for other nanocomposite systems such as polyimide/organoclay, nylon 6/organoclay and PCL/organoclay nanocomposites in which better dispersion of organoclay resulted in higher tensile property [29-31].

Tab. 3. Mechanical properties of EVA nanocomposites.

Composition	Morphology	Young's modulus [MPa]	Elongation at break [%]	Tensile strength [MPa]	Yield stress [Mpa]
EVA	-	43 ± 1,1	820 ± 22	25 ± 0,5	5,6 ± 0,2
EVA + Nanofil 15	Intercalated	54 ± 1,3	663 ± 15	17 ± 0,6	5,6 ± 0,2
EVA + P-Nanofil15	Intercalated	60 ± 1,9	715 ± 17	19 ± 0,8	5,8 ± 0,3
EVA + Somasif MEE	Exfoliated	62 ± 1,7	721 ± 18	20 ± 0,8	6,1± 0,3
EVA + P-Somasif MEE	Exfoliated	82 ± 2,0	644 ± 35	21 ± 1,1	7,7 ± 0,3

A difference in the aspect ratio between Nanofil 15 and Somasif MEE may however contribute to the difference in their affect on tensile properties. It is interesting to observe that the Young's modulus follow the same trend observed for the yield stresses τ_0 of nanocomposites. This behavior has been recently discussed and quantified and it can be also attributed to the size and shape of the nanoparticles in the polymeric matrix [27].

The purification of organoclays led to nanocomposites with better tensile properties as compared to original commercial organoclays. For example in the intercalated nanocomposite, purification of Nanofil 15 increases the improvement of the elastic modulus over EVA from 26% to 40%. A reduction of negative effects of clay on elongation at break and tensile strength is simultaneously observed. For example, elongation at break reduces by 13% with P-Nanofil 15 instead of 20% with the original organoclay.

All the nanocomposites exhibit lower ultimate tensile strength values, associated to lower elongation at break. This behavior is probably due to both the presence of some defects in the macromolecular structure (e.g. not intercalated nanoclays) and the hindering effect of intercalated/exfoliated nanoclays that prevents the complete alignment of polymer chains.

Improvements are more evident in the case of the exfoliated nanocomposites. Indeed upon purification of Somasif MEE, elastic modulus increases by 100% over that of EVA as compared to 44% with commercial Somasif. In this case reduction of elongation at break (12%) is less affected by increase of modulus as compared to the intercalated nanocomposite which increases up to 21%.

Finally the yielding point of the nanocomposite EVA - P-Somasif MEE was higher than all the other systems suggesting the presence of better interactions between the polymeric matrix and the organoclay platelets. The mechanical properties of polymer-clay nanocomposites depend both on degree of dispersion of the clay platelets in the polymer matrix and on the clay matrix interactions. The impurities adsorbed on the organoclay can negatively affect the interaction between clay and polymer which is responsible for the improvement of mechanical properties in the nanocomposites. Moreover the products of thermal degradation of the clay organic modifier (see above [9, 10]) which may occur on polymer-clay melt blending can be partially retained at the polymer clay interface by their delayed volatilization and thus affect the mechanical properties of the nanocomposites. The temperature used here for EVA-organoclays melt blending (125°C-130°C) is below the range of temperature for decomposition of the surfactants (>200°C, Figure 1). However it is possible that the local temperature experienced in the extruder by the compound undergoing heavy shear stress, reaches the temperature for decomposition of unconfined surfactant (200°C-250°C). The improvement observed in the mechanical properties of the nanocomposites prepared with washed organoclay could be due to the absence in this case of residual products of unconfined clay which determins the clay-polymer interaction.

Conclusions

Purification of organoclays does affect the mechanical properties of EVA nanocomposites when the purified organoclays are melt-compounded. Indeed, as the washing process eliminates the impurities and completely confines the surfactant within the clay layers increasing its thermal stability; mechanical properties such as Young modulus are also improved. According to the rheological measurements the washing procedure improves the degree of clay dispersion.
The improvement of mechanical properties is more evident for the exfoliated nanocomposites. Indeed if the improvement in modulus for EVA – Nanofil 15 intercalated nanocomposites with the purified clay is of about 50% larger with respect to that with the untreated clay (17MPa compared to 11MPa), for EVA – Somasif MEE exfoliated nanocomposites, the improvement is of 100% (39MPa

compared to 19MPa). Moreover the nanocomposites prepared with purified Somasif MEE showed an increase of the tensile yield stress.
It is also noticeable that nanocomposites prepared with purified organoclays show a lower reduction of elongation at break relative to modulus increase as compared to original commercial clays.

References

[1] Okada A.; Kasumi M.; Usuki A.; Kojoma Y.; Kurauchi T.; Kamigaito O.; *Mater. Res. Soc. Proc.* **1990**, *171*, 40.
[2] Messersmith P.B.; Giannelis E.P.; *Chem. Mater.* **1994**, *6*, 1719.
[3] Fischer H.R.; Gielgens L.H.; Koster T.P.; *Acta Polymerica* **1999**, *50*, 122.
[4] Messersmith P.B.; Giannelis E.P.; *J. of Polym. Sci.: Part A Polym. Chem.*, **1995**, *33*, 1047.
[5] Gieseking J.E. *Soil. Sc.,i* **1939**; 47: 1.
[6] Xie W.; Gao Z.; Liu K.; Pan W.; Vaia R.; Hunter D.; Singh A.; *Thermochimica Acta*, **2001**, *367-368*, 339.
[7] Zilg C.; Thomann R.; Finter J.; Mülhaupt R.; *Macromol. Mater. Eng.*, **2000,** *280*, 41.
[8] Morgan A.B.; Harris J.D.; *Polym.*, **2003**, *44*, 2313.
[9] Xie W.; Gao Z.; Pan W.; Hunter D.; Singh A.; Vaia R.; *Chem. Mater.*, **2001**, *13*, 2789.
[10] Davis R.D.; Gilman J.W.; Sutto T.E.; Callahan J.H.; Trulove P.C.; De Long H.C.; *Clay and Clay Minerals*, **2004**, *52*, 171.
[11] Zanetti M.; Camino G.; Reichert P.; Mülhaupt R.; *Macromol. Rapid Commun.*, **2001**, *22*, 176.
[12] Zanetti M.; Camino G.; Thomann R.; Mülhaupt R.; *Polymer*, **2001**, *42*, 4501.
[13] Zanetti M.; Kashiwagi T.; Falqui L.; Camino G.; *Chemistry of Materials*, **2002**, *14*, 881.
[14] Pastore H.O.; Frache A.; Boccaleri E.; Marchese L.; Camino G.; *Macromol. Mater. Eng.*, **2004**, *289*, 783.
[15] Wagener R.; Reisinger T.J.G.; *Polymer*, **2003**, *44*, 7513.
[16] Krishnamoorti R.; Vaia R.A.; Giannelis E.P.; *Chem. Mater.*, **1996,** *8*, 1728, 34.
[17] Krishnamoorti R.; Giannelis E.P.; *Macromol.*, **1997**, 30, *4097*,102.
[18] Ren J.; Silva A.S.; Krishnamoorti R.; *Macromol.*, **2000**, *33*, 3739, 46.
[19] Krishnamoorti R.; Ren J.; Silva A.S.; *J. Chem. Phys.*, **2001**,*114*, 4968, 73.
[20] Solomon M.J.; Almusallam A.S.; Seefeldt K.F.; Somwhangthanaroj A.; *Macromol. Rapid. Commun.*, **2001**, *22*, 519, 23.
[21] Lim Y.T.; Park O.O.; *Rheol. Acta*, **2001**, *40*, 220, 9.
[22] Galgali G.; Ramesh C.; Lele A.; *Macromol.*, **2001**, *34*, 852, 8.
[23] Hyun Y.H.; Lim S.T.; Choi H.J.; Jhon M.S.; *Macromol.*, **2001**, *34*, 8084, 93.
[24] Krishnamoorti R.; Mitchell C.A.; *J. Polym. Sci. B*, **2002**, *40*, 1434, 43.
[25] Lim S.T., Hyun Y.H., Choi H.J., and Jhon M.S., *Chem. Mater.*, **2002** 14, 1839.
[26] Lim S:T:, Lee C.H. , Kim H.B., Choi H.J., Jhon M.S. *e-Polymers*, **2004**, no.026.
[27] Krishnamoorti R., Yurekli K. *Curr Opin Colloid Interface Sci* **2001**, *6(5–6),* 464.
[28] Vlasveld D.P.N., De Jonga M., Berseec H.E.N., Gotsisa A.D., Picken S.J., *Polymer* **2005**, *46*, 10279.
[29] Chang J.H.; Park K.M.; Cho D.; *Polym. Eng. Sci.*, **2001**, *41*, 1514.
[30] Dennis H.R.; Hunter D.L.; Chang D.; Kim S.; White J.L.; Cho J.W.; Paul D.R.; *Polymer*, **2001**, *42*, 9513.
[31] Di Y.; Iannace S.; Sanguigno L.; Nicolais L.; *Macromol. Symp.*, **2005**, *228*, 115.